# Directional Variations in Surface Roughness Determinations

## 측정방향에 따른 표면 거칠음 정도의 변화 양상

Lee, Seok - Won*
이 석 원

## 요 지

여러 연구들을 통하여 표면 거칠음 정도가 접촉면 전단력에 매우 중요함이 밝혀졌으며, 따라서 그 역할을 충분히 이해하기 위해서는 표면 거칠음 정도가 정확히 정량화 되어져야 한다. 현재까지 이러한 표면 거칠음 정도를 나타내는 표면 거칠기 매개변수는 대부분 방향성을 고려하지 않은 3차원적인 trisector에서 측정되어 왔고, 그 결과는 정적인 표면을 대표하는 값으로 적당하였다. 그러나, 표면 거칠기 매개변수와 접촉면 전단력과 같이 방향성을 갖는 매개변수와의 상관관계를 조사하기 위해서는 전단방향과 동일한 방향으로 측정된 2차원적인 표면 거칠음 값이 더욱더 합리적인 대표 값이 될 수 있다. 따라서, 본 연구에서는 전단방향을 고려한 표면 거칠음 정도를 구할 수 있는 새로운 표면 거칠기 매개변수를 제안하였다. 제안된 방향성 매개변수와 기존의 표면 거칠기 매개변수를 비교 분석함으로서, 방향성 매개변수와 비 방향성 매개변수와의 상관관계를 조사하였다. 표면 거칠음 정도는 디지털 이미지 분석 시스템을 이용한 Optical Profile Microscopy(OPM) 방법을 이용하여 측정하였다. 그 결과, 본 연구에서 측정된 여러 가지 표면 거칠기 매개변수는 측정값에 있어서 비슷한 경향을 보여주었으며, 따라서, 서로간의 상관관계가 좋음이 밝혀졌다. 또한 표면 거칠음 정도가 증가함에 따라, 비 방향성의 3차원 매개변수 값이 방향성의 2차원 매개변수보다 계속적으로 증가하는 양상이 보여졌다.

## Abstract

It was found that surface roughness has a first-order effect on the interface shear strength and accordingly it should be accurately quantified if its role is to be properly understood. Most of the surface roughness parameters are based on the trisector approach (three dimensional parameter) which can provide a good measure of the surface roughness from a static perspective. However, if roughness is to be correlated with a directional sensitive parameter such as interface shear then a two dimensional parameter could be more meaningful if the roughness measurements are made parallel to the direction of shearing. In this paper, alternative roughness parameters which consider the direction of shearing are described. These directional parameters are compared with the existing roughness parameters, and

* Member, Senior Researcher, Korea Institute of Construction Technology

the relationship between these directional and non-directional parameters are investigated. The surface roughness was quantified by using the Optical Profile Microscopy (OPM) method (Dove and Frost, 1996) based on the digital image analysis. The results showed that the various surface roughness parameters measured in this study exhibit similar trend of roughness values, so that, good relationships are obtained between these roughness parameters. As the surface roughness increases, the roughness values measured in trisector coupons are increasing higher than those measured in parallel coupons.

**Keywords** : Surface roughness, Geomembrane, Interface, Digital image analysis, Shear

## 1. Introduction

It was found that surface roughness has a first-order effect on the interface shear strength and accordingly it should be accurately quantified if its role is to be properly understood. To quantify the surface roughness, Gokhale and Drury (1990), for example, used three vertical cross sections oriented at 120 degrees to each other and found that the results would yield an error of less than six percent over a completely random sampling of a large number of sections on the most highly anisotropic surface. Based on Gokhale and Drury's theoretical developments, Dove and Frost (1996) developed the Optical Profile Microscopy (OPM) method for determining the profile roughness parameter, $R_L$, and the surface roughness parameter, $R_S$, for geomembranes. The surface roughness parameters were obtained from measurements on three profiles oriented at 120 degrees to each other to capture any anisotropy which may exist.

This means that the individual profile measurements are not necessarily aligned with the shear direction. Conceptually, the three dimensional parameter, $R_S$, which is based on the trisector approach provides a good measure of the surface roughness from a static perspective, however, if roughness is to be correlated with a directional sensitive parameter such as interface shear then a two dimensional parameter, such as $R_L$ could be more meaningful if the roughness measurements are made parallel to the direction of shearing.

In this paper, alternative roughness parameters which consider the direction of shearing are described. These directional parameters are compared with the existing roughness parameters, and the relationship between these directional and non-directional parameters is investigated. A brief review of the OPM method selected to measure surface roughness in this study is described.

## 2. Surface Roughness Parameters Measured in This Study

### 2.1 Normalized Roughness Parameter, $R_n$

Uesugi and Kishida (1986) found that the interface shear strength between soils and machined steel surfaces was influenced by the surface roughness of the material, the $D_{50}$ of the sand, and the interaction

of these factors. Based on this, they concluded that the surface roughness could be better correlated with interface shear strength when normalized by the sand particle size. They suggested that the normalized roughness parameter, $R_n$, be defined as follows:

$$R_n = \frac{R_{max}(L = D_{50})}{D_{50}} \tag{1}$$

where; $R_{max}$ $(L = D_{50}) = R_{max}$ when $L = D_{50}$,
$D_{50}$ = mean grain size, and
L = gauge length of $R_{max}$.

## 2.2 Profile Roughness Parameter, $R_L$ and Surface Roughness Parameter, $R_S$

Based on the theoretical developments of Gokhale and Underwood (1990) and the experimental work of Gokhale and Drury (1990), Dove and Frost (1996) proposed the Optical Profile Microscopy (OPM) method to quantify the surface roughness of geomembranes.

For a two-dimensional profile of a material surface, the profile roughness parameter, $R_L$ is defined as:

$$R_L = \frac{L}{L_0} \tag{2}$$

where; L = the actual length of the profile, and
$L_0$ = the projected length of the profile.

For a three-dimensional surface, the surface roughness parameter, $R_S$ is defined as:

$$R_S = \frac{A_S}{A_0} \tag{3}$$

where; $A_S$ = the actual area of the surface, and
$A_0$ = the projected area of the surface.

For most practical applications, the three-dimensional surface roughness, $R_S$ can be accurately derived from two-dimensional profile roughness, $R_L$ based on stereology as:

$$R_S = \overline{R_L \phi} \tag{4}$$

where, $\phi$ is the profile structure factor as defined by Gokhale and Drury (1990) as:

$$\phi = \int_0^{\pi} [\sin\alpha + [\frac{\pi}{2} - \alpha]\cos\alpha] f(\alpha, \phi)\, d\alpha \tag{5}$$

where, $\alpha$ is the angle from vertical of a line segment on the profile and $\varphi$ is the orientation of the normal to a vertical sectioning plane with respect to a reference axis. The quantity $f(\alpha, \varphi)$ is the frequency distribution function of the line segment orientations over all two-dimensional profiles of the

surface which provides information on the distribution of surface topography. Further details on the derivation is provided by Gokhale and Drury (1990), Dove and Frost (1996), and Lee (1999).

## 3. Experimental Procedures

A series of roughness measurements on virgin and previously used geomembranes were performed using the digital image analysis based Optical Profile Microscopy (OPM) technique (Dove and Frost, 1996). This method permits profiling a wide range of geomembrane surfaces. The used geomembranes were taken from specimens on which interface shear tests between geotextiles and geomembranes had been performed. The virgin geomembranes were taken from the same roll of geomembrane that the used geomembrane specimens were taken from but were not used in any shear testing before their surface were quantified.

### 3.1 Geomembranes Evaluated

One smooth and three textured HDPE geomembranes which are considered to be representative of the range of textures and texture patterns presently available to designers were analyzed in this study. Photographs of each geomembrane were provided by Lee (1999). Geomembranes used were:

- NSC Dura Seal HD geomembrane: represents the "smooth" geomembrane manufactured by National Seal Co. This geomembrane has a very glossy surface.
- GSE Friction Flex geomembrane: represents the "slightly textured" geomembrane manufactured by GSE Lining Technology, Inc. This has the least relief of the textured samples used in this study.
- NSC Friction Seal geomembrane: represents the "moderately textured" geomembrane manufactured by National Seal Co. This is the most highly anisotropic of the samples studied. The texture of this geomembrane is composed of rows of texture elements oriented in the cross machine direction with the surface between the texture elements being relatively smooth. The texture of the geomembrane surface was made by the extrusion coating technique in which a flat sheet coat hanger die is used to extrude a coating onto the surface of a previously made and tested smooth geomembrane (Donaldson, 1994).
- Poly-Flex Textured geomembrane: represents the "moderately/heavily textured" geomembrane manufactured by Poly-Flex, Inc. This geomembrane has the most relief of the textured samples used in this study. The texture of this geomembrane was made by the blown coextrusion technique (Donaldson, 1994).

### 3.2 Preparation of Coupons for Optical Profile Microscopy(OPM) Method

Procedures for preparing coupons for study using the OPM method were similar to those developed by Dove (1996). Fig. 1 shows a plan view of the sectioning planes and their orientations. Five coupons were obtained: three parallel to the shear direction, and two oriented at 120 degrees to the shear direction. Typically, the second sectioning line was chosen as the reference axis and was aligned parallel to the machine direction and shear direction. Coupons 1, 2, and 3 were designated as the Parallel Coupons, and Coupons 2, 4, and 5 were designated as the Trisector Coupons.

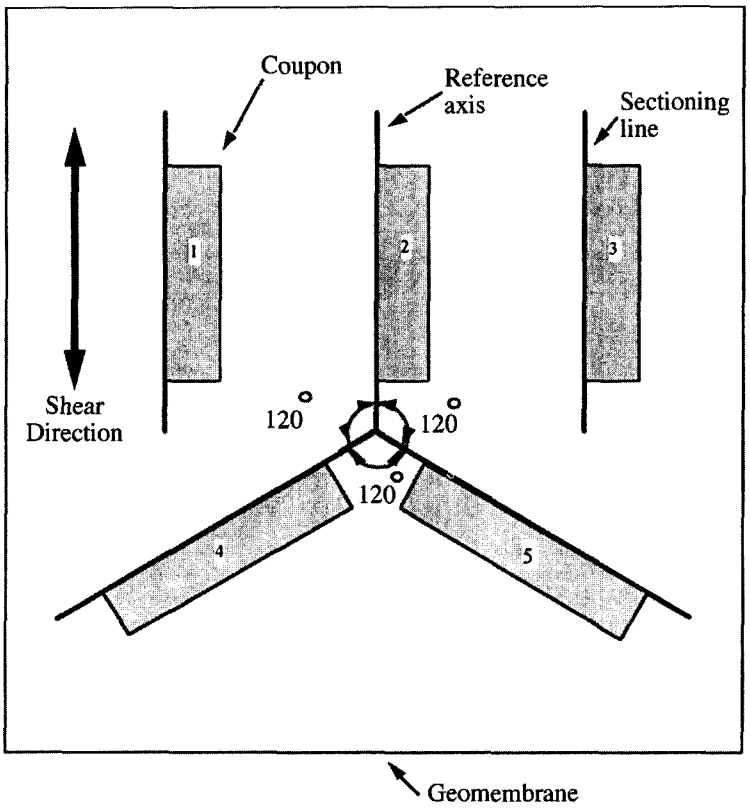


Fig. 1. Vertical sectioning planes and orientations

These coupons were embedded in a Plaster of Paris mixture having a cement to water ratio of 2.5:1. Plaster of Paris mixture was used in this study to enhance the contrast between the black geomembranes and the white background material, thereby yielding clearer images for subsequent measurements using image analysis. The sample molds consisted of circular plastic petri dishes with diameters of 90 mm and depths of 18 mm. The geomembrane specimens had lengths of 60 mm and heights of 15 mm. Air entrapped in the Plaster of Paris paste after it was poured in the mold was removed by tapping the mold on a flat surface.

Once a petri dish had been filled with Plaster of Paris, coupons were inserted on their edges through the paste with the cross section of interest placed firmly against the petri dish bottom. The surface of interest was then denoted as side A. Care was taken to insert the coupons as vertically as possible.

After the Plaster of Paris material containing the coupons had hardened, the plastic petri dish was peeled away leaving a circular disk of material with a smooth base. Consecutive grinding and polishing of the smooth base was conducted to expose the geomembrane coupons using a commercial grinder/polisher apparatus. 120 grit sand paper and then 240 grit sand paper were used during grinding to expose the geomembrane coupons without damaging the specimen. Polishing cloth was then used to sharpen the boundary between the Plaster of Paris and the geomembrane. Fig. 2 provides an example schematic of a completed disk showing the five coupons exposed for imaging.

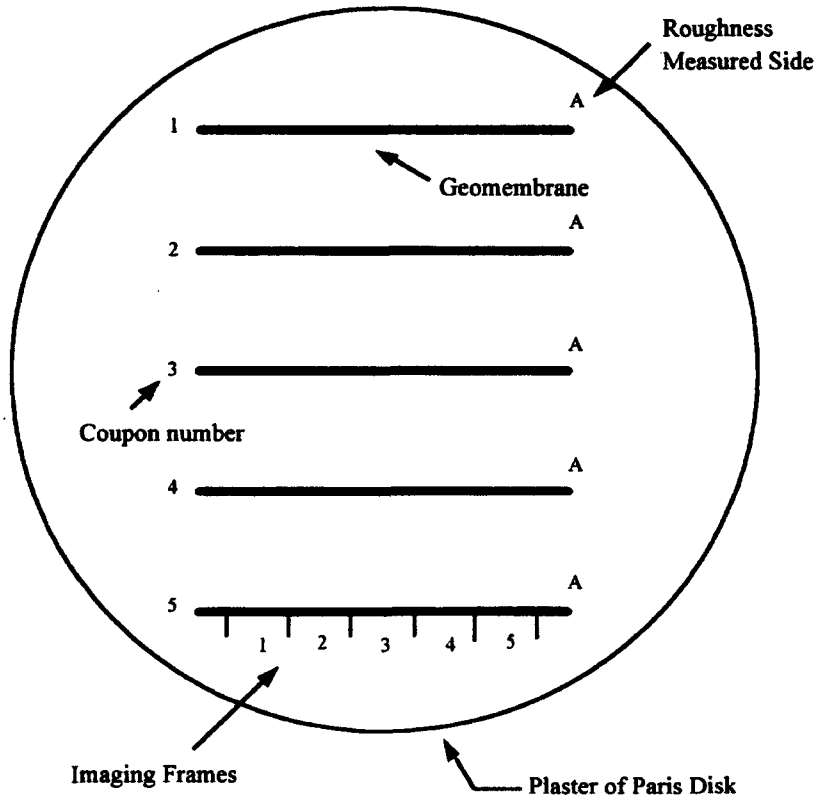


Fig. 2. Bottom view of completed disk

## 3.3 Digital Image Analysis

All image analyses in this study were performed on a Cambridge Instruments, Leica Quantimet Q-570 image analyzer. The system has a resolution of 512 pixels horizontally by 480 pixels vertically. Details of the systems and imaging methods used in this study can be found in Frost and Kuo (1996) and Dove and Frost (1996).

An important consideration in profiling is the selection of the appropriate magnification level and sufficient measuring length. As shown by Dove and Frost (1996), the magnification was chosen to represent the 7 mm of geomembrane profile by 512 pixels on the computer screen which was considered sufficiently sensitive to the range of roughness used in this study. At this magnification, each imaging frame was 7 mm in length, so that each parameter was determined by the profile length of 105 mm (7 mm × 5 images × 3 coupons) which was shown to be sufficient to obtain an accurate roughness value (Dove and Frost, 1996).

## 3.4 Data Acquisition

Once a gray image was captured by the CCD camera attached to the microscope, the binary image

was extracted through the process of detection which applies thresholds to the gray image. The surface profile of the geomembrane was then obtained by using the outline command which leaves only a single line of pixels representing the common boundary between background and geomembrane. Since the outline of only the side of geomembrane, denoted A, against which the shear strength test was conducted, was needed for determining the roughness value, the pixels making up the outline of the side not being examined and the two image boundaries were erased from the image using the binary image editing functions of the analyzer. The measurements of each parameter were then conducted based on the procedures proposed by Dove and Frost (1996).

# 4. Results

## 4.1 Geomembrane Roughness Determinations

As noted above, both virgin and used geomembrane roughness values were quantified in this study. Using the procedure described above, the following roughness parameters were measured:

- Parallel Profile Roughness Parameter ($R_{L,P}$): the profile roughness parameter ($R_L$) from the parallel coupons;
- Trisector Profile Roughness Parameter ($R_{L,T}$): the profile roughness parameter ($R_L$) from the trisector coupons;
- Surface Roughness Parameter ($R_S$): the surface roughness parameter ($R_S$) from the trisector coupons;
- Parallel Normalized Roughness Parameter ($R_{n,P}$): the normalized roughness parameter ($R_n$) from the parallel coupons;
- Trisector Normalized Roughness Parameter ($R_{n,T}$): the normalized roughness parameter ($R_n$) from the trisector coupons.

Table 1 presents the results obtained for virgin geomembranes of various roughness parameters including the means, standard deviations, and coefficients of variation.

As seen in Table 1, $R_S$ values for textured virgin geomembranes range from 1.24 to 1.77, and appropriately represent the degree of texturing. The $R_{L,P}$ values also reflect the degree of texturing and range from 1.19 to 1.59. It is observed that $R_n$ values ($R_{n,P}$ and $R_{n,T}$) for the textured virgin geomembranes, however, show limited variation ranging from 0.16 to 0.38 for $R_{n,P}$ and 0.17 to 0.44 for $R_{n,T}$. These small ranges of variation may not be sufficient to permit distinction between roughness values for certain conditions.

Table 2 presents the results obtained from used geomembranes of various roughness parameters. It is noted that Table 2 includes roughness measurements made after different numbers of shear tests had been conducted, thus, the means, the standard deviations, and the coefficients of variation are not included. A similar trend is found for the used geomembrane surface roughness determinations to those for virgin geomembranes. $R_S$ and $R_{L,P}$ represent the degree of texturing appropriately, however, the various $R_n$ values ($R_{n,P}$ and $R_{n,T}$) exhibit narrow ranges.

Roughness values measured after the first shear test are summarized in Table 3 along with their means, the standard deviations, and the coefficients of variation. It is observed that the variations of roughness determinations are strongly dependent on the manufacturing methods of geomembrane surface textures.

Table 1. Results of surface roughness determinations of virgin geomembranes

| Manufacturer | Product | Membrane Number | Statistics | Parallel | | Trisector | | |
|---|---|---|---|---|---|---|---|---|
| | | | | $R_{L,P}$ | $R_{n,P}$ | $R_{L,T}$ | $R_S$ | $R_{n,T}$ |
| GSE Lining Technology Inc. | Friction Flex | 2.2 | | 1.21 | 0.18 | 1.22 | 1.27 | 0.19 |
| | | 2.6 | | 1.19 | 0.16 | 1.19 | 1.24 | 0.17 |
| | | | Mean | 1.20 | 0.17 | 1.21 | 1.25 | 0.18 |
| National Seal Co. | Friction Seal HD | 3 | | 1.59 | 0.38 | 1.64 | 1.77 | 0.41 |
| | | 5 | | 1.37 | 0.27 | 1.38 | 1.46 | 0.30 |
| | | 9 | | 1.43 | 0.29 | 1.59 | 1.73 | 0.41 |
| | | 11 | | 1.31 | 0.24 | 1.42 | 1.51 | 0.31 |
| | | 17 | | 1.36 | 0.27 | 1.42 | 1.52 | 0.32 |
| | | | Mean | 1.41 | 0.29 | 1.49 | 1.60 | 0.35 |
| | | | Standard Deviation | 0.11 | 0.05 | 0.12 | 0.14 | 0.06 |
| | | | Coefficient of Variation | 0.08 | 0.17 | 0.08 | 0.09 | 0.17 |
| Poly-Flex, Inc. | Textured HDPE | 4 | | 1.49 | 0.32 | 1.49 | 1.59 | 0.34 |
| | | 8 | | 1.45 | 0.29 | 1.61 | 1.73 | 0.40 |
| | | 12 | | 1.50 | 0.32 | 1.55 | 1.67 | 0.39 |
| | | 22 | | 1.49 | 0.33 | 1.61 | 1.74 | 0.42 |
| | | 10 | | 1.49 | 0.32 | 1.63 | 1.77 | 0.44 |
| | | | Mean | 1.48 | 0.31 | 1.58 | 1.70 | 0.40 |
| | | | Standard Deviation | 0.02 | 0.02 | 0.06 | 0.07 | 0.03 |
| | | | Coefficient of Variation | 0.01 | 0.06 | 0.04 | 0.04 | 0.08 |

Table 2. Results of surface roughness determinations of used geomembranes

| Manufacturer | Product | Membrane Number | Parallel | | Trisector | | |
|---|---|---|---|---|---|---|---|
| | | | $R_{L,P}$ | $R_{n,P}$ | $R_{L,T}$ | $R_S$ | $R_{n,T}$ |
| National Seal Co. | Dura Seal HD (smooth) | 1 | 1.07 | 0.06 | 1.07 | 1.09 | 0.06 |
| GSE Lining Technology Inc. | Friction Flex | 2 | 1.20 | 0.17 | 1.19 | 1.24 | 0.17 |
| | | 2.1 | 1.20 | 0.17 | 1.23 | 1.28 | 0.20 |
| | | 2.2 | 1.17 | 0.14 | 1.20 | 1.24 | 0.18 |
| | | 2.3 | 1.17 | 0.16 | 1.17 | 1.21 | 0.16 |
| | | 2.4 | 1.20 | 0.17 | 1.19 | 1.23 | 0.17 |
| | | 2.5 | 1.20 | 0.18 | 1.23 | 1.28 | 0.20 |
| | | 2.6 | 1.17 | 0.15 | 1.19 | 1.23 | 0.17 |
| National Seal Co. | Friction Seal HD | 3 | 1.32 | 0.26 | 1.38 | 1.45 | 0.27 |
| | | 5 | 1.32 | 0.25 | 1.25 | 1.30 | 0.21 |
| | | 7 | 1.32 | 0.27 | 1.42 | 1.52 | 0.33 |
| | | 9 | 1.35 | 0.28 | 1.32 | 1.39 | 0.25 |
| | | 11 | 1.33 | 0.25 | 1.40 | 1.49 | 0.30 |
| | | 13 | 1.41 | 0.32 | 1.47 | 1.58 | 0.36 |
| | | 15 | 1.37 | 0.25 | 1.38 | 1.45 | 0.25 |
| | | 17 | 1.35 | 0.28 | 1.41 | 1.51 | 0.32 |
| | | 19 | 1.41 | 0.28 | 1.45 | 1.55 | 0.30 |
| | | 21 | 1.30 | 0.23 | 1.38 | 1.46 | 0.30 |
| Poly-Flex, Inc. | Textured HDPE | 4 | 1.32 | 0.24 | 1.40 | 1.49 | 0.30 |
| | | 6 | 1.34 | 0.25 | 1.42 | 1.52 | 0.33 |
| | | 8 | 1.41 | 0.29 | 1.52 | 1.63 | 0.36 |
| | | 10 | 1.46 | 0.29 | 1.56 | 1.68 | 0.37 |
| | | 12 | 1.43 | 0.25 | 1.53 | 1.65 | 0.38 |
| | | 14 | 1.52 | 0.31 | 1.60 | 1.73 | 0.40 |
| | | 16 | 1.40 | 0.28 | 1.42 | 1.51 | 0.31 |
| | | 18 | 1.57 | 0.32 | 1.71 | 1.87 | 0.46 |
| | | 20 | 1.40 | 0.28 | 1.52 | 1.64 | 0.43 |
| | | 22 | 1.31 | 0.25 | 1.48 | 1.60 | 0.39 |
| | | 23 | 1.46 | 0.28 | 1.61 | 1.74 | 0.41 |
| | | 24 | 1.57 | 0.33 | 1.71 | 1.86 | 0.47 |

Table 3. Average roughness values after first shear test

| Manufacturer | Product | Statistics | Parallel | | Trisector | | |
|---|---|---|---|---|---|---|---|
| | | | $R_{L,P}$ | $R_{n,P}$ | $R_{L,T}$ | $R_S$ | $R_{n,T}$ |
| GSE Lining Technology Inc. | Friction Flex | | 1.20 | 0.17 | 1.23 | 1.28 | 0.20 |
| | | | 1.17 | 0.16 | 1.17 | 1.21 | 0.16 |
| | | | 1.20 | 0.17 | 1.19 | 1.23 | 0.17 |
| | | | 1.20 | 0.18 | 1.23 | 1.28 | 0.20 |
| | | | 1.17 | 0.15 | 1.19 | 1.23 | 0.17 |
| | | Mean | 1.19 | 0.17 | 1.20 | 1.25 | 0.18 |
| | | Standard Deviation | 0.02 | 0.01 | 0.03 | 0.03 | 0.02 |
| | | Coefficient of Variation | 0.01 | 0.08 | 0.02 | 0.02 | 0.12 |
| National Seal Co. | Friction Seal HD | | 1.32 | 0.27 | 1.42 | 1.52 | 0.33 |
| | | | 1.33 | 0.25 | 1.40 | 1.49 | 0.30 |
| | | | 1.41 | 0.32 | 1.47 | 1.58 | 0.36 |
| | | | 1.37 | 0.25 | 1.38 | 1.45 | 0.25 |
| | | | 1.35 | 0.28 | 1.41 | 1.51 | 0.32 |
| | | | 1.41 | 0.28 | 1.45 | 1.55 | 0.30 |
| | | | 1.30 | 0.23 | 1.38 | 1.46 | 0.30 |
| | | Mean | 1.36 | 0.27 | 1.42 | 1.51 | 0.31 |
| | | Standard Deviation | 0.04 | 0.03 | 0.04 | 0.05 | 0.03 |
| | | Coefficient of Variation | 0.03 | 0.11 | 0.02 | 0.03 | 0.10 |
| Poly-Flex, Inc. | Textured HDPE | | 1.46 | 0.29 | 1.56 | 1.68 | 0.37 |
| | | | 1.43 | 0.25 | 1.53 | 1.65 | 0.38 |
| | | | 1.52 | 0.31 | 1.60 | 1.73 | 0.40 |
| | | | 1.40 | 0.28 | 1.42 | 1.51 | 0.31 |
| | | | 1.57 | 0.32 | 1.71 | 1.87 | 0.46 |
| | | | 1.40 | 0.28 | 1.52 | 1.64 | 0.43 |
| | | | 1.46 | 0.28 | 1.61 | 1.74 | 0.41 |
| | | | 1.57 | 0.33 | 1.71 | 1.86 | 0.47 |
| | | Mean | 1.48 | 0.29 | 1.58 | 1.71 | 0.40 |
| | | Standard Deviation | 0.07 | 0.02 | 0.10 | 0.12 | 0.05 |
| | | Coefficient of Variation | 0.05 | 0.08 | 0.06 | 0.07 | 0.13 |

For example, it is noted that the National Seal Friction Seal HD has a higher standard deviation than the Poly-Flex Textured geomembrane for the virgin geomembrane even though its average roughness value is smaller. However, the roughness values after the first shear test indicate that the National Seal Friction Seal HD has a lower standard deviation than the Poly-Flex Textured geomembrane. This is due to the differences in the manufacturing of geomembrane surface textures. The National Seal Friction Seal HD has an easily breakable surface texture. Part of the surface texture of this geomembrane might have been damaged during the manufacturing, packing (rolling for transportation), and unpacking of the geomembrane. This may be the cause for the greater variations in roughness values measured for the virgin geomembranes. The remaining easily breakable surface texture can be easily removed during the

first shear test, thus consistent surface texture throughout the geomembrane specimen can be achieved. Consequently, smaller standard deviation is achieved than Poly-Flex Textured geomembrane after first shear test. In addition, the National Seal Friction Seal HD has rows of texture elements oriented in the cross machine direction with a relatively smooth zone in between. This variability in the manufacturing process produces the most highly anisotropic structure and results in the largest coefficient of variation of the geomembranes used in this study.

## 4.2 Comparison of Various Roughness Parameters

Fig. 3 and Fig. 4 show the relationship between $R_n$ ($R_{n,P}$ and $R_{n,T}$) and $R_L$ ($R_{L,P}$ and $R_{L,T}$), and $R_{n,T}$ and $R_S$ for both used and virgin geomembranes, respectively. Fig. 3 includes both parallel and trisector measurements, however, Fig. 4 includes only measurements from the trisector coupons since $R_S$ can only be measured for trisector coupons. Good relationships are shown in both cases for the geomembrane textures examined in this study. This means that various roughness parameters measured in this study exhibit similar trends of roughness values even though the ranges of roughness value are different. For practical purposes, the following relationships are suggested.

$$R_L = 1.409 \times R_n + 1.0 \tag{6}$$

$$R_S = 1.701 \times R_{n,T} + 1.0 \tag{7}$$

It is noted that if the surface is perfectly smooth (flat), the value of $R_n$ is 0 and $R_L$ and $R_S$ are 1.0, thus Equations of 6 and 7 have the offset of 1.0. It is also noted that the $R_n$ values measured in this study were normalized by the size of geotextile fiber diameter. Different sizes of polymer fibers could

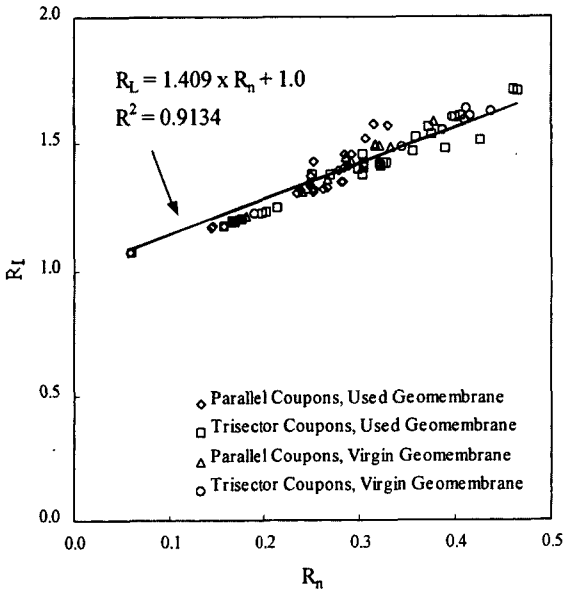


Fig. 3. Relationship between $R_n$($R_{n,T}$, $R_{n,P}$) and $R_L$($R_{L,T}$, $R_{L,P}$)

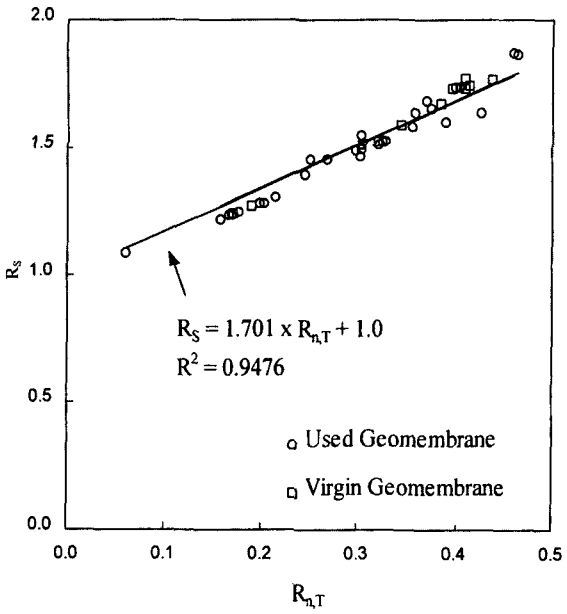


Fig. 4. Relationship between $R_{n,T}$ and $R_S$

change the values of $R_n$ slightly and therefore affect the relationships shown in Equations 6 and 7.

Since the $R_S$ parameter (stereology based $R_S$) described in Session 2 required a determination of the profile structure factor, $\phi$, to estimate the $R_S$ from the measurements of $R_L$, use of the roughness parameter, $R_S$ may not always be attractive particularly where rapid determination is desirable. Underwood and Banerji (1987) presented the following semi-empirical expression for the rapid determination of $R'_S$, suitable for all partially oriented surfaces. The advantage of this equation is that it permits estimation of $R'_S$ from determination of $R_L$ only.

$$R'_S = \frac{4}{\pi}(R_L - 1.0) + 1.0 \tag{8}$$

The values of $R_S$ based on the stereology (stereology based $R_S$) are compared with the values obtained using Equation 8 ($R'_S$), as shown in Fig. 5 for both used and virgin geomembranes. The 45 degree line represents agreement of the computed values to those obtained on the basis of the stereology and the dashed lines represent the 95 percent confidence interval of the values. The $R'_S$ values determined in Equation 8 are always within the 95 percent confidence interval of the values obtained on the basis of the stereology, and overestimate the roughness very slightly for the geomembrane textures used in this study.

*For rapid practical determination of $R_S$ from $R_L$, the new semi-empirical expression ($R''_S$)* is derived by relating the stereology based $R_S$ with $R'_S$ measured in this study as shown in Fig. 5 and Equation 9. This relationship could be used to correlate the data for stereology based $R_S$ and could give the preliminary roughness values of $R''_S$ directly from $R_L$. The following equation is suggested.

$$R''_S = 0.958 \times (R'_S - 1.0) + 1.0 \tag{9}$$

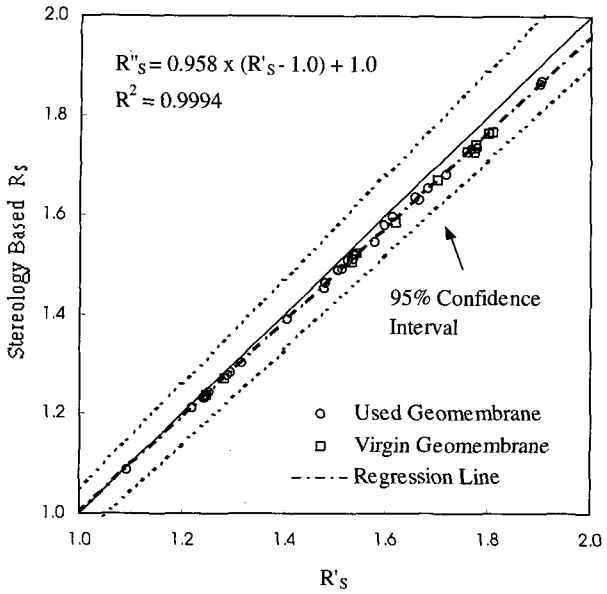


Fig. 5. Comparison of R'S and stereology based RS values

This makes use of the surface roughness parameter attractive in field quality assurance procedures where rapid determination of $R_S$ are desirable. However, it is presently recommended that Equation 9 be used only for the range of geomembrane textures examined in this study. Geomembranes of other texture patterns should be fully characterized by the stereology based method.

### 4.3 Comparison of Roughness Determinations between Parallel and Trisector Coupons

Fig. 6 and Fig. 7 present the comparisons of parallel and trisector coupons for $R_L$ and $R_n$, respectively. It is noted that as the surface roughness increases, the roughness values measured in trisector coupons are increasingly higher than those measured in parallel coupons.

Fig. 8 presents the comparison of parallel and trisector $R_L$ ($R_{L,P}$ and $R_{L,T}$) with $R_S$. Clearly, it can be seen that the $R_{L,T}$ shows better relationship with $R_S$ since both $R_S$ and $R_{L,T}$ values come from same coupons (trisector coupons). $R_{L,P}$, however, shows somewhat larger amount of scatter in the relationship with $R_S$, since the values of $R_{L,P}$ come from different coupons.

## 5. Conclusions

This study introduced alternative roughness parameters which consider the direction of shearing. These directional parameters have been compared with the existing roughness parameters. The following conclusions are based on the data and interpretation presented in this study:

1) Both the directional parameter, $R_{L,P}$ and nondirectional parameter, $R_S$ values appropriately reflect the degree of texturing for the geomembranes used in this study, however, $R_n$ values (both $R_{n,P}$ and $R_{n,T}$) showed limited ranges of variation which may not be sufficient to permit distinction between

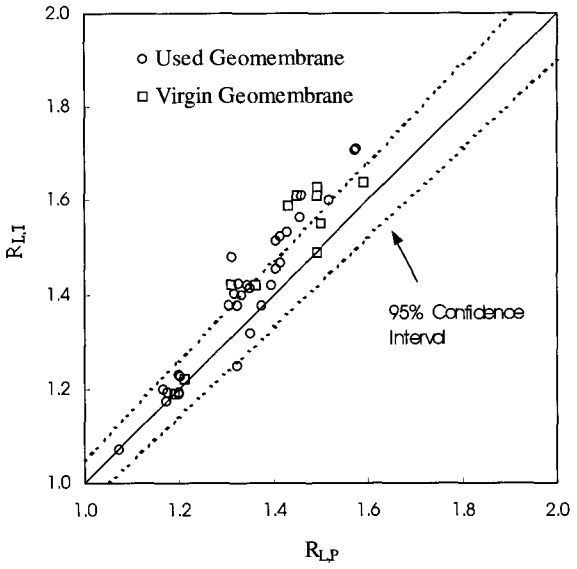


Fig. 6. Comparison of parallel and trisector $R_L$

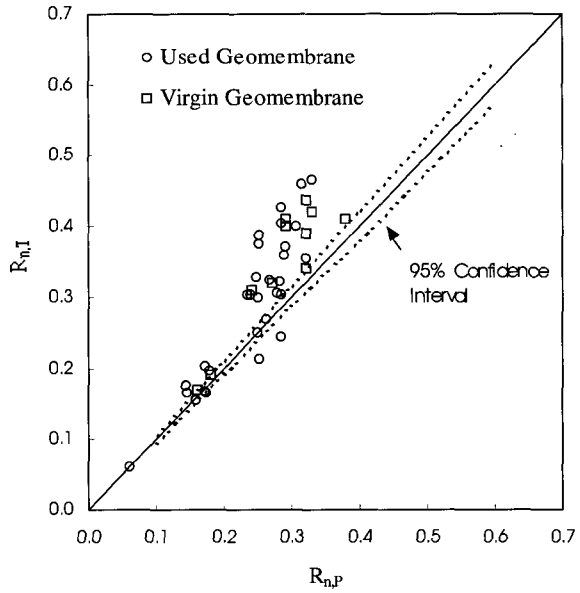


Fig. 7. Comparison of parallel and trisector $R_n$

roughness values for certain conditions.

2) The various surface roughness parameters measured in this study ($R_{L,P}$, $R_{L,T}$, $R_S$, $R_{n,P}$, and $R_{n,T}$) exhibit similar trend of roughness values, so that, good relationships are obtained between these roughness parameters.
3) As the surface roughness increases, the roughness values measured in trisector coupons are increasing higher than those measured in parallel coupons.

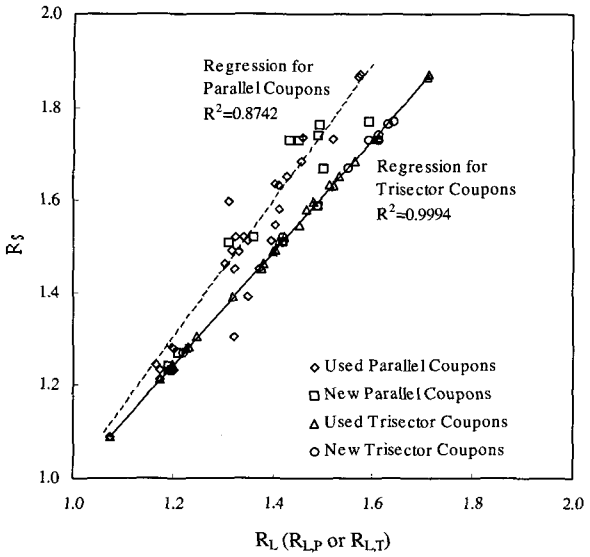


Fig. 8. Comparison of parallel and trisector $R_L$ with $R_S$

4) It is found that both directional parameter, $R_{L,P}$ and non-directional parameter, $R_S$, could be efficient roughness parameters to relate with the interface shear strength.

It is noted that the general observations found in this study are based on the results of geomembrane texture and texture patterns examined in this study. Geomembranes of other texture patterns should be fully investigated.

## References


1. Donaldson, J. J., (1994), "Texturing Techniques, In: Geosynthetic Resins, Formulations and Manufacturing, Edited by Koerner, R. M.", Proceedings of a Seminar Held at the Geosynthetic Research Institute, Drexel University, Philadelphia, PA, pp. 113~122.
2. Dove, J. E., (1996), "Particle-Geomembrane Interface Strength Behavior as Influenced by Surface Topography", Ph.D. Dissertation, School of Civil and Environmental Engineering, Georgia Institute of Technology.
3. Dove, J. E., and Frost, J. D., (1996), "A Method for Measuring Geomembrane Surface Roughness", Geosynthetics International, Vol. 3, No. 3, pp. 369~392.
4. Frost, J. D., and Kuo, C. Y., (1996), "Automated Determination of the Distribution of Local Void Ratio from Digital Images", Geotechnical Testing Journal, GTJODJ, Vol. 19, No. 2, June, pp. 107~117.
5. Gokhale, A. M., and Underwood, E. E., (1990), "A General Method for Estimation of Fracture Surface Roughness: Part I. Practical Considerations", Metallurgical Transactions A, Vol. 21A, pp. 1201~1207.
6. Gokhale, A. M., and Drury, W. J., (1990), "A General Method for Estimation of Fracture Surface Roughness: Part II. Theoretical Aspects", Metallurgical Transactions A, Vol. 21A, pp. 1193~1199.
7. Lee, S. W., (1999), "Quantification of Surface Topography Using Digital Image Analysis", Journal of the Korean Geotechnical Society, Vol. 15, No. 3, June, pp. 131~149.
8. Uesugi, M., and Kishida, H., (1986), "Frictional Resistance at Yield Between Dry Sand and Mild Steel", Soils and Foundations, JSSMFE, Vol. 26, No. 4, Dec., pp. 139~149.
9. Underwood, E. E., and Banerji, K., (1987), "Quantitative Fractography", In: Metals Handbook, Vol. 12, ASM, Metal Park, OH, pp. 193~210.


(접수일자 1999. 5. 27)